Nonenzymatic Hydration of Phosphoenolpyruvate: General Conditions for Hydration in Protometabolism by Searching Across Pathways

Authors: Joris Zimmermann[1], Atalay Bora Basar[1], and Joseph Moran[1,2,3]*

[1] Institut de Science et d'Ingénierie Supramoléculaires (ISIS), CNRS UMR 7006, Université de Strasbourg 8 Allée Gaspard Monge,67000 Strasbourg (France)

[2] Institut Universitaire de France (IUF) (France)

[3] Department of Chemistry and Biomolecular Sciences, University of Ottawa, Ottawa, Ontario, K1N 6N5, Canada

Corresponding author E-mail: moran@unistra.fr

Abstract: Numerous reactions within metabolic pathways have been reported to occur nonenzymatically, supporting the hypothesis that life began from a primitive nonenzymatic precursor to metabolism. However, most of those studies reproduce individual transformations or segments of pathways without providing a common set of conditions for classes of reactions that span multiple pathways. In this study, we search across pathways for common nonenzymatic conditions for a recurring chemical transformation in metabolism: alkene hydration. The mild conditions that we identify (Fe oxides such as green rust) apply to all hydration reactions of the rTCA cycle and gluconeogenesis, including the hydration of phosphoenolpyruvate (PEP) to 2-phosphoglycerate (2PGA), which had not previously been reported under nonenzymatic conditions. Mechanistic insights were obtained by studying analogous substrates and through anoxic and radical trapping experiments. Searching for nonenzymatic conditions across pathways provides a complementary strategy to triangulate conditions conducive to the nonenzymatic emergence of a protometabolism.

Main Text: Life is a complex chemical system and identifying the processes leading to its emergence is one of the most challenging problems in science. Self-organized complex systems are created when a specific group of repeating mechanisms interact with each other. The "metabolism-first hypothesis" is an approach to understanding the origin of life[1–10] that suggests that the initial stage of life's development involved a complex network of self-organized chemical reactions made up of repeating chemical mechanisms that were driven by geological processes on the early Earth. Indeed, biological metabolism features a repeating set of chemical mechanisms, consistent with this idea. As the number of mechanisms found in the core of metabolism is restrained, and since many other downstream functions depend on their continuous operation, the extent to which the core of metabolism might change appears to be highly limited. Indeed, comparing modern autotrophic microbial metabolisms with those inferred to be operating in the last universal common ancestor (LUCA) indicates very little change to the structure and mechanisms of metabolism over roughly 4 billion years.[10] For the same reasons, the main chemical mechanisms and reactions found in the core of metabolism may bear strong similarities to those in the original prebiotic network.

Towards the goal of recreating the origin of life in the lab within the metabolism-first framework, our group is attempting to infer the environment under which self-organized chemistry began by systematically searching for conditions under which the most conserved parts of the anabolic network occur in the absence of enzymes. Over the past decade, we and others have reported numerous reactions within metabolic pathways that occur in the presence of inorganic promoters.[11–26] However, most of these studies reproduce individual transformations or reaction segments within a single pathway without providing a common set of conditions for classes of reactions that span multiple pathways. Searching across metabolic pathways for conditions that enable a recurring chemical mechanism would offer a complementary search strategy that could help pinpoint conditions of broader relevance to the origins of metabolism.

Alkene hydration (and its mechanistic reverse, alcohol dehydration) is a reaction mechanism that occurs three times within the rTCA cycle (known as the reverse Krebs cycle),[27] an autocatalytic pathway that produces life's universal organic building blocks for biosynthesis[28] (Fig. 1A). Within this cycle, fumarate is hydrated to malate whereas aconitate undergoes hydration to citrate or to isocitrate. The hydration reactions converting fumarate (**1b**) to malate (**3a**) and, aconitate (**1c**) to citrate (**4a**) and isocitrate (**4b**) are thermodynamically favorable (-3.57, -8.49, and -2.38 kJ/mol, respectively[29]) and involve an iron-sulfur cluster as a co-factor.[30,31] The mechanism proceeds through the *anti*-addition of a water molecule across the double bond of fumarate or aconitate by fumarase or aconitase, respectively.[32] Alkene hydration also occurs once within gluconeogenesis, the pathway that life uses to build the sugar-phosphate backbone that becomes incorporated into nucleic acids. The alkene within the enol moiety of phosphoenolpyruvate (**PEP**, **1a**) undergoes hydration to form 2-phosphoglycerate (**2PGA, 2a**).[33] Unlike the hydration reactions in the rTCA cycle, the biological hydration of **PEP** to **2PGA** is not thermodynamically favorable (+2.8 kJ/mol[34]) and does not involve a Lewis acid Fe-S cluster; instead, Mg^{2+} catalysis is used.[33,35]

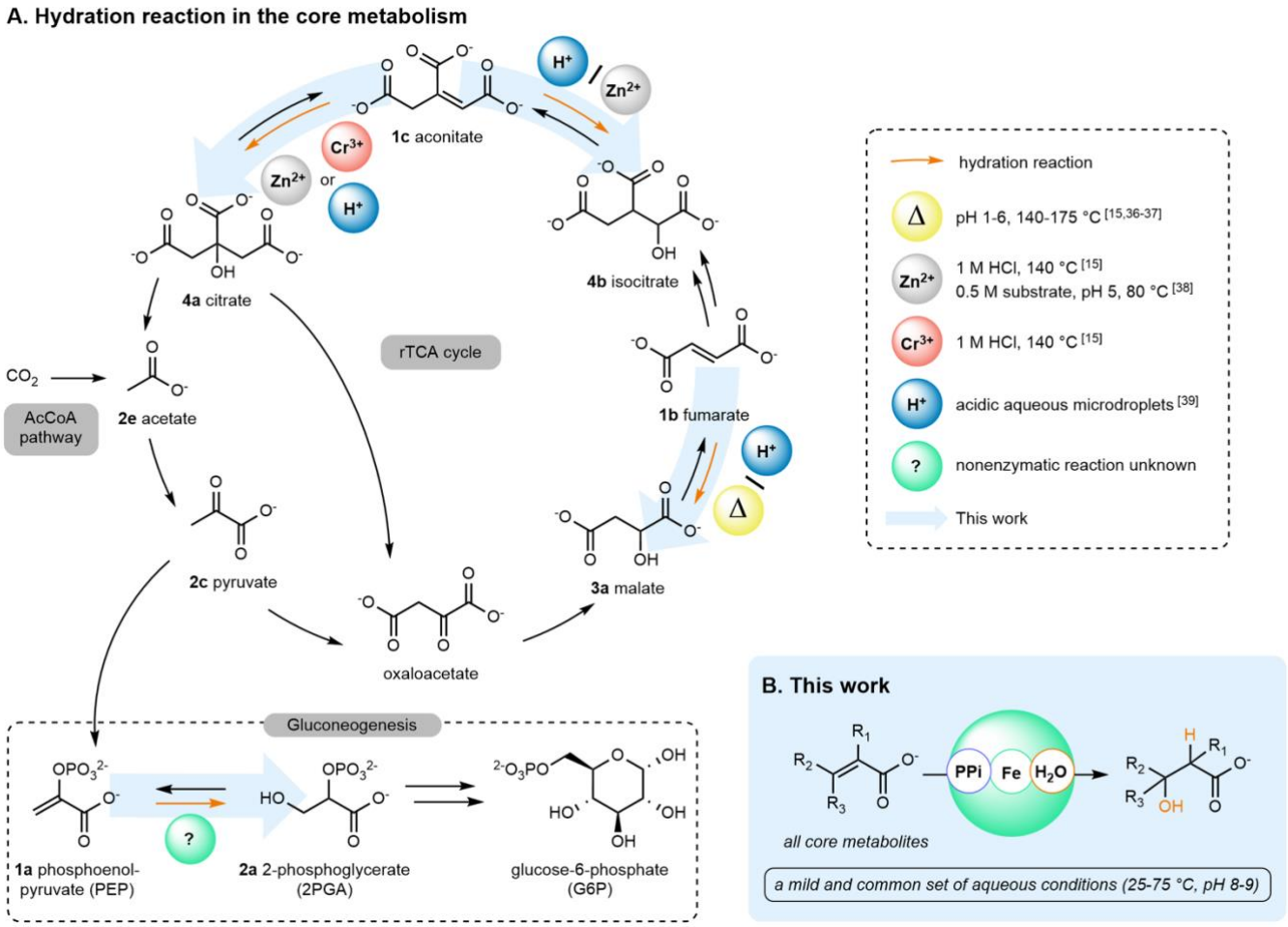

Figure 1. (A) Hydration reactions in core metabolism and the different reports of this nonenzymatic transformation, notably lacking the hydration of **PEP** to **2PGA**. (B) This work, in which a common set of mild aqueous conditions is suitable for the hydration of all core metabolites in the figure.

Some of the metabolic hydration reactions described above have been reported to occur under nonenzymatic conditions, albeit under quite different ones, whereas the hydration of **PEP** to **2PGA** has not yet been reported (Fig. 1A). For example, the hydration of fumarate to malate was found to occur in acidic conditions (pH 1-6) at elevated temperatures (125-200 °C) without metal catalysts.[15,36,37] The conversion of aconitate to isocitrate was promoted by Zn^{2+} ions in highly acidic conditions (1 M HCl) at elevated temperature (140 °C)[15] or in concentrated and acidic conditions (0.5 M substrate, pH 5) at 80 °C.[38] Similarly, the conversion of aconitate to citrate was shown to proceed in highly acidic conditions (1 M HCl) under Cr^{3+} catalysis at elevated temperatures (140 °C).[15] Alternatively, aqueous microdroplets generated under high-pressure nebulization were found to hydrate fumarate to malate and to hydrate aconitate to a mixture of isocitrate and citrate at the air-water interface,[39] which was found to be highly acidic.[40] However, highly acidic conditions, especially those rich in metal ions, are not compatible with the hydration of **PEP** to **2PGA** since **PEP** readily hydrolyses to pyruvate under those conditions.[41–43] Here, we search across pathways for common nonenzymatic conditions for alkene hydration and identify mild, unified conditions that apply to all hydration reactions of the rTCA cycle and gluconeogenesis (Fig. 1B), including, for the first time, the hydration of **PEP** to **2PGA**. Interestingly, the conditions empirically identified through a broad screen are environments previously predicted to be of high interest for the origin of metabolism (mildly alkaline aqueous

conditions containing Fe oxides such as green rust).[3,44] These results help constrain the search for conditions for the emergence of a nonenzymatic metabolism-like reaction network.

Results and Discussion

Nonenzymatic hydration of PEP to 2PGA

We began our investigation by screening for conditions that allowed for the nonenzymatic hydration of **PEP** to **2PGA**. **PEP** (**1a**) hydrolyzes to pyruvate (**2c**) under acidic conditions (pH 1-7),[41] and thus alkaline pH values were expected to be more suitable. We screened a series of metals using $NaHCO_3$ to buffer the reaction at pH 8-9 under air for 24 h at 60 °C (for details see Table S1 and Fig. S10), quenching the reaction by precipitating metals with a thiolate/phosphate solution prior to ^{1}H NMR analysis. Of the 15 combinations of metals in various oxidation states that were screened, characteristic signals of **2PGA** (**2a**) were observed in trace amounts only when iron metal or ferrous iron salts were used (Fig. S12). Notably, Cr^{3+} or Zn^{2+}, which are known to catalyze nonenzymatic hydration reactions under acidic conditions,[15,38,45,46] or Fe^{3+} were ineffective. We next evaluated the influence of organic and inorganic ligands on the iron metal (Fe^0) or iron (II) chloride (Fe^{2+}) promoted reaction, screening at 75 °C for 16 h (Fig. 2A-B, for details, see Table S2). Polyphosphates significantly improved the formation of **2a** (Fig. 2B). Most notably, starting the reaction with Fe^0 (1 equiv.) and pyrophosphate (2 equiv.), **2a** was formed in 16% yield, as determined by quantitative ^{1}H NMR (for details, see Table S2). No reaction was observed when pyrophosphate was used in the absence of Fe^0. When starting the reaction from Fe^{2+} (1 equiv.) and pyrophosphate (2 equiv.), **2a** was formed in 8% yield. Without polyphosphates or in the presence of any other organic or inorganic ligands, yields <2% were obtained (Fig. 2B, left) and significant amounts of precipitated iron salts were observed at the end of the reaction (Table S2). Phosphate ligands possess a high affinity for iron ions[47,48] and polyphosphates are known to prevent iron precipitation,[49–51] for example by ligating iron ions released from the oxidation of Fe^0.[49]

We noticed that the conditions that promoted the hydration reaction were very similar to those needed for the formation of green rust. In $NaHCO_3$ solutions, green rust can be formed from metallic iron (Fe^0) in a deep-green homogeneous layer that covers the metallic surface.[52] A chloride green rust sample was therefore independently prepared from a mixture of Fe^{2+} and Fe^{3+} and tested in our standard conditions (under air, 75 °C, 16 h) to verify that the reaction could occur in the presence of such naturally abundant minerals. In this case, the formation of **2a** was detected in up to 10% yield in the presence of pyrophosphate (for details, see Table S8 entry 7-8). Further experiments related to green rust are described in the next section.

For subsequent optimization, conditions starting from Fe^0 were employed since these gave the best yields of **2a.** By decreasing the temperature to 60 °C, 40 °C, or 25 °C after a reaction time of 16 h, **2a** was observed in 15%, 11%, and 4% yields, respectively (Fig. 2B, right, for details, see Table S4). By increasing the reaction time to 6 days, the yield obtained of **2a** did not significantly change when the reaction was run at 40 °C and 60 °C but slightly increased at 25 °C and 75 °C to 11% and 21% yields, respectively. Subsequent experiments were therefore performed at 75 °C.

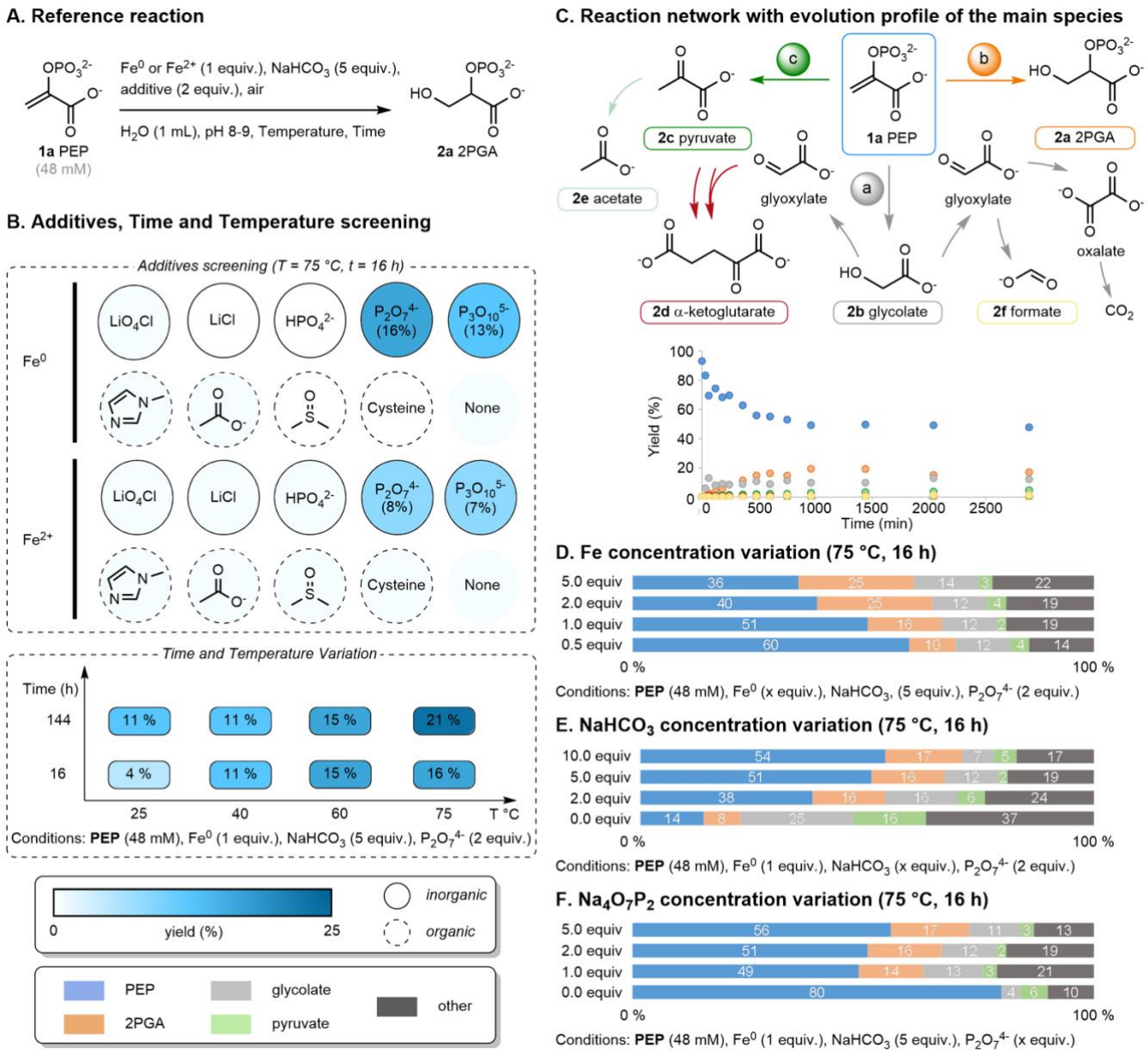

Figure 2. (A) Reference reaction. (B) Additives, time, and temperature screening. (C) Reaction network and the associated quantitative evolution of the main species in the reaction (for details, see Table S7). Concentration variations with the quantification of the main species, including **1a** (blue), **2a** (orange), **2b** (grey), and **2c** (green) in the reaction with unaccounted mass balance given in black with the component varied: (D) Fe, (E) $NaHCO_3$ and (F) $Na_4O_7P_2$.

To gain further insight into the mass balance and mechanism, a series of identical reactions were quenched at different times by precipitating metals using a thiolate/phosphate solution and examined by ^{1}H and ^{31}P NMR (for details, see Table S7). Three main products were identified after quenching the reaction: **2a**, glycolate (**2b**), and pyruvate (**2c**) (Fig. 2C). During the first hour of the reaction, mostly **2b** is formed (13% yield). After a 1 h induction period, **2a** starts to form over 16 h, accompanied by a corresponding decrease in the concentration of **1a** (50% of **1a** recovered, Fig. 2C). Along with these two main pathways, we identified the formation of a few additional minor species like α-ketoglutarate (**2d**), acetate (**2e**), and formate (**2f**) (Fig. 2C, for details, see Table S7). To understand the mechanism of formation of these side products, we resubjected **2a**, **2b,** and **2c** to the standard conditions (i.e., **Fe^0** (1 equiv.), $Na_4P_2O_7$ (2 equiv.), and $NaHCO_3$ (5 equiv.)). Starting from either of these three compounds, only

trace amounts of **2e** and **2f** were detected (Fig. S17-19). When the reaction was started from **2b**, it was found to partially oxidize to glyoxylate (Fig. 2C, see also Fig. S18). **2d** was recently reported to form through a reductive aldol condensation between **2c** and glyoxylate.[15,53,54] Therefore, the formation of **2d** is explained by the in situ formation of glyoxylate and **2c** from **2b** and **1a**, respectively (Fig. S20).

We next investigated how the different reaction parameters could influence the formation of the main products (Fig. 2D-F, for details, see Table S5). The quantification of the main species, including **1a** (blue), **2a** (orange), **2b** (grey), and **2c** (green), is represented in Fig. 2D-F, with unaccounted mass balance given in black. When the concentration of Fe^0 was doubled from 1 to 2 equiv., the yield of **2a** increased from 16% to 25% but without a further notable improvement when 5 equiv. of Fe^0 was used (Fig. 2D). Notably, increasing the equiv. of Fe^0 increased the yield of **2a** but not of **2b** or **2c**. However, when the amount of Fe^0 was decreased to 0.5 equiv., the yield of **2a** was also decreased to 10%. The formation of **2a** appears linked to the equiv. of Fe^0, whereas **2b** and **2c** are not. Increasing the concentration of $NaHCO_3$ did not significantly affect the reaction whereas decreasing the amount of $NaHCO_3$ from 5 to 2 to 0 equiv. considerably increased the yields of side products **2c** (increasing from 3-4% to 16%) and **2b** (increasing from 12% to 25%) while decreasing the yield of **2a** (decreasing from 16% down to 8%) (Fig. 2E). We evaluated the importance of the $Na_4O_7P_2$ concentration (Fig. 2F). As previously mentioned, by removing $Na_4O_7P_2$ from the reaction conditions, the yield of **2a** was decreased to trace amounts as well as lower yields of **2b**. However, decreasing the equivalents of $Na_4O_7P_2$ from 2 to 1 or increasing from 2 to 5 had little influence on the outcome. We note that in Figs. 2D-F, the missing mass balance (10-37%) is accounted for by the other side products in Fig. 2C and by the unavoidable loss of metabolites within precipitates or on surfaces (for details, see Table S7).

Next, the influence of the pH in buffer solutions was investigated. The reaction is pH dependent, requiring a pH ≥ 6; otherwise, the hydrolysis pathway is favored (60% yield of **2c**, Table S6). Finally, the concentration of **1a** was decreased from 48 mM to 10 mM without changing the concentration of the other parameters of the reaction (i.e., Fe^0 (48 mM), $NaHCO_3$ (240 mM) and $Na_4O_7P_2$ (96 mM)). In that case, **2a** was formed in 21% yield while **2b** and **2c** were observed in 27% and 3% yields, respectively (Table S5 entry 11).

Investigation of the promoter of the reaction

The observations that 1) **2b** is immediately formed in the reaction, 2) **2a** only begins to be formed after an induction period of 1 h, and 3) **2a** and **2b** are not derived from each other suggests that their formation from **1a** follows two independent mechanisms. As all reactions were thus far carried out under air, we wondered whether O_2 reduction might be involved in the formation of one of both products. Indeed, in the presence of iron species, O_2 can be reduced to H_2O_2 forming iron oxides in solution which can further form hydroxyl radicals via the Fenton reaction.[55–58] Since the formation of **2b** was previously reported from the degradation of **1a** under a variety of oxidative conditions,[59] we first tried mixing **1a** with H_2O_2 (1 equiv.) in the absence of metal under our standard conditions and indeed observed the formation of **2b** but not **2a** (Fig. 3, see also Fig. S21). Given reports of epoxidation of alkenes by H_2O_2 in $NaHCO_3$ solution,[60] we propose that epoxidation of **1a** is followed by hydrolysis of the epoxide[61] and subsequent elimination of phosphate to form hydroxypyruvate, which undergoes oxidative

decarboxylation to give **2b** (Fig. S22B). To verify this hypothesis, hydroxypyruvate was subjected to the oxidative reaction conditions and the standard conditions using Fe^0. In both cases, **2b** was formed after 2 h at 75 °C (Fig. 3, for details, see Fig. S22A). Product **2b** therefore appears to be a direct result of O_2 reduction under the reaction conditions.

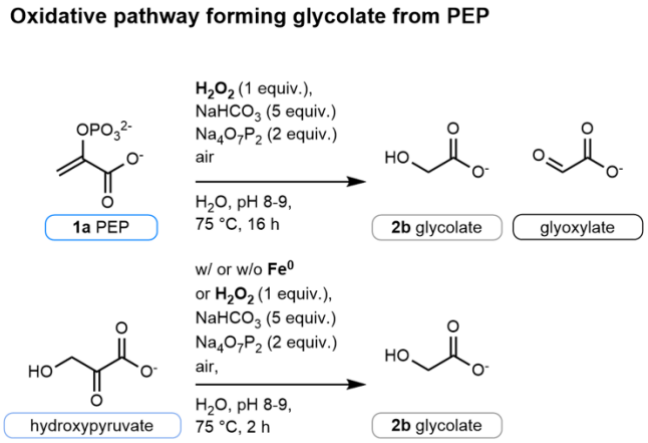

Figure 3. Investigation of the formation of glycolate (**2b**). Two control experiments were performed in which **2b** is formed.

To get more insights and define key parameters regarding the formation of **2a**, additional experiments were performed. In the lab, green rust can be produced from the oxidation of metallic iron, by the oxidation of Fe(II) species, or by mixing Fe(II) and Fe(III) salts. Carbonate green rust oxidizes into α-FeO(OH) (goethite) or transforms into Fe_3O_4 (magnetite) when left in solution.[62,63] We tested the influence of α-FeO(OH) or Fe_3O_4 on the reaction but did not observe the formation of **2a** in either case (Table S8, entries 9-10). Starting the reaction with Fe^{3+} was ineffective, whereas the addition of a reducing agent such as Zn^0 in the same mixture promoted the formation of **2a** in 5% yield (Table S8, entry 2), highlighting the need for iron oxides of mixed oxidation state generated under air.

To investigate whether O_2 is involved in the formation of the active promoter, the reaction was carried out starting from Fe^0, from Fe^{2+}, or from preformed green rust in an anaerobic environment (Fig. 4A, see Table S9). In the case of Fe^0 or Fe^{2+}, the experiments only produced **2a** and **2b** in trace amounts while no product was observed in the case of green rust. To investigate whether radical species (e.g., derived from the Fenton reaction) are involved in the formation of **2a**, we performed the reaction under air in the presence of the radical scavenger 2,2,6,6-tetramethylpiperidinyloxy (TEMPO, 1 equiv.). In this case, only trace amounts of **2a** was detected while **2b** was still formed in 8% yield (Fig. 4B, see Table S10). This experiment suggests that an open-shell species is involved in the formation of **2a**. Considering that **2b** forms immediately in the presence of H_2O_2 even without Fe whereas **2a** forms only in the presence of Fe after a 1 h induction period, the formation of **2a** likely depends not only on the presence of a radical (possibly hydroxyl radical), but also on the slow formation of a reactive iron species.

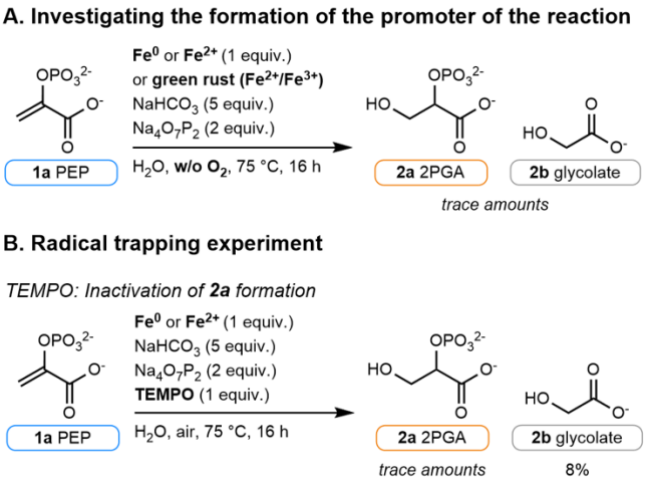

Figure 4. (A) Investigating the formation of the active promoter of the reaction under an inert nitrogen atmosphere. (B) Radical trapping experiments using TEMPO. Quantification of the products by ^{1}H qNMR (for details, see Table S10).

Hydration of other metabolites

The hydration conditions were applied to other common metabolites found in core metabolism (Fig. 5). Unlike **1a**, most of the other hydration reactions in core metabolism do not act on a terminal alkene. Fumarate (**1b**), a symmetric alkene, underwent hydration to malate (**3a**) in 20% and 19% yields after 16 h at 40 °C or 75 °C, respectively (Table S11). Next, we studied the hydration of aconitate (**1c**), whose alkene is not symmetric and thus presents two potential sites of hydration. By quenching a series of identical reactions at different times, we observed the formation of citrate (**4a**) by ^{1}H NMR along with a mixture of diastereoisomers of isocitrate (**4b**), the three potential hydration products of **1c**, again forming only after a 1 h induction period (Fig. S26). After a reaction time of 16 h at 40 °C, 22% of hydrated products were obtained with **4b** as the major product (19%, mixture of diastereoisomers, Table S12) and **4a** as the minor product (3% yield). The hydrated products **3a**, **4a** and **4b** could also be observed at 25 °C, but lower yields were obtained in that case (Table S11-S12). From the hydration of **1c**, side products **2c** (3% yield, Table S12, entry 3) and **2e** were also observed, which could be formed through the retro-aldol reaction of **4a** to **2e** and oxaloacetate, which decarboxylates to **2c** (Fig. 6). Indeed, when **4a** was subjected to our standard conditions, **2c** and **2e** were detected, whereas this was not the case when starting from **4b** (Table S13, see also Fig. S28A-B). To support the intermediacy of oxaloacetate in this process, we set out to trap it using Zn^{0} by reducing it to malate (**3a**) prior to decarboxylation to **2c**. When **4a** was subjected to standard conditions at 40 °C in the presence of 5 equiv. of Zn^{0}, **3a** was observed in 1% yield in addition to **2c**, and **2e** (Table S13, see also Fig. S28C). This result is notable as it shows that these conditions are compatible not only with all the hydration reactions in the rTCA cycle and gluconeogenesis but also with the retro-aldol reaction in the rTCA cycle, a nonenzymatic reaction that had been previously observed only in aqueous microdroplets generated under high pressure.[39]

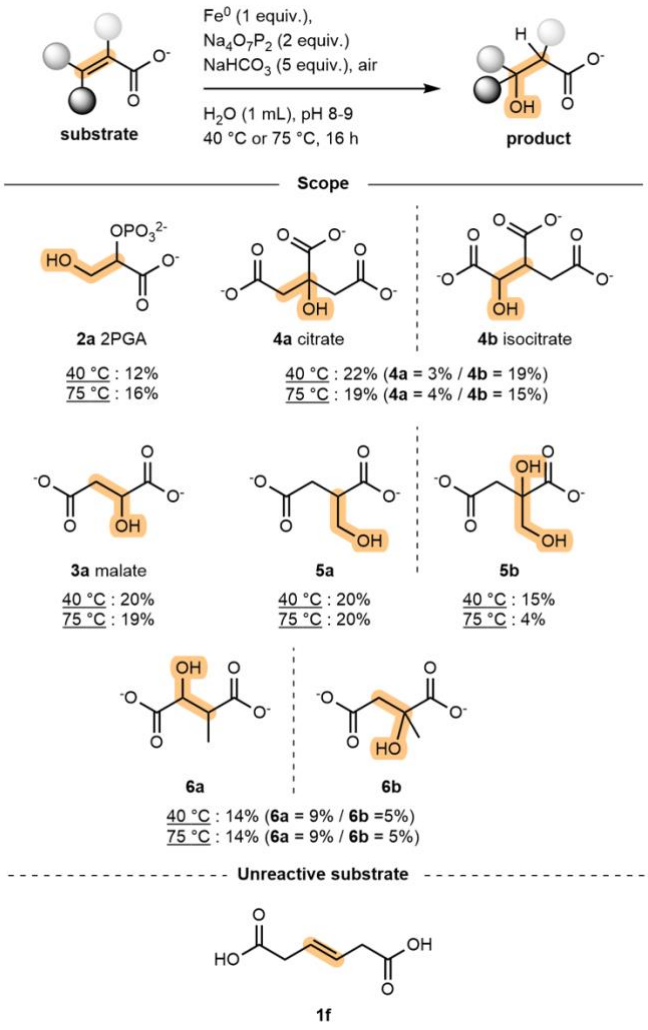

Figure 5. Scope of the reaction. Quantification of the product by ^{1}H qNMR (for details, see Table S11-S16).

The regioselectivity of hydration was investigated. Itaconate (**1d**), which features a terminal alkene, and mesaconate (**1e**), were used as model substrates in our standard conditions (Fig. 5). In the hydration of **1d**, like that of **1a**, we observed an exclusive oxa-Michael hydration with formation of **5a** in 20% yield (for details, see Table S14). Moreover, we identified the formation of a dihydroxylation side product (**5b,** Fig. S29) in 15% yield (after 16 h at 40 °C), which might, like **2b**, have been formed from epoxidation followed by hydrative ring-opening. Subjecting **1e** to our standard conditions gave a mixture of hydration regioisomers **6a** and **6b** in 14% combined yield in a 9:5 ratio, favoring hydration at the least substituted site (for details, see Table S15 and Fig. S30). The influence of the position of the carboxylate group relative to the alkene was evaluated. Attempts to hydrate diacid **1f** were unsuccessful, emphasizing the importance of conjugation between alkene and carboxylate (Fig. 5, for details, see Table S16).

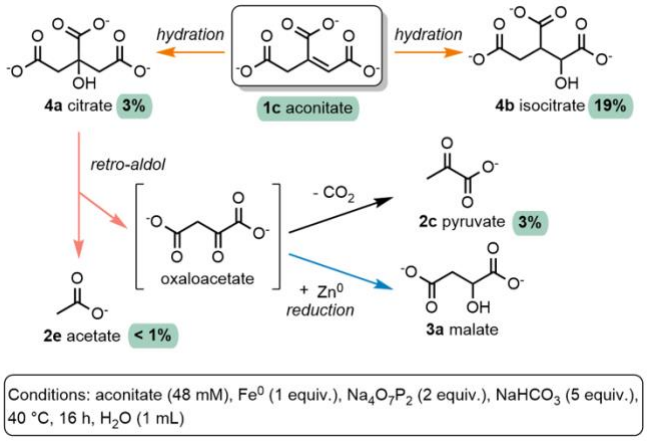

Figure 6. Hydration of aconitate and retro-aldol of citrate under a common set of conditions. The products were quantified by ^{1}H qNMR (for details, see Table S13). Oxaloacetate is not stable under the standard conditions but can be trapped using Zn^{0} as a reducing agent (blue arrow), in which case malate **3a** was observed when starting from citrate **4a**.

Finally, we tested the ability of the various hydration reactions to occur in the same environment, and their potential competition (Fig. 7). When a mixture of **1a**, **1b,** and **1c** at similar concentrations was subjected to our standard conditions (48 mM, 1 equiv. of **Fe^{0}**), we observed the formation of **2a**-**2e**, **3a** and **4a**-**4b** by ^{1}H NMR (Fig. S32). The hydrated products were obtained in 5% yield each for **2a**, **3a,** and **4b** while **4a** was formed in 1% yield for a total of 16% yield of hydrated products (Table S17, entry 1). Moreover, when we increased the equivalents of **Fe^{0}** from 1 to 3, the ratio between the different hydrated products did not change significantly. In this case, **2a**, **3a**, and **4a** were formed in 8%, 11%, and 9% yields while **4b** was formed in 2% yield; 30% overall yield (Table S17, entry 2). These experiments demonstrate the existence of a continuous (in the sense of happening at the same time in a one-pot manner[64]) reaction network involving several different classes of transformations, including hydration (formation of **2a**; **3a**, **4a,** and **4b**), dehydration (formoyl formate to fumaroyl formate), aldol (glyoxylate and **2c** to formoyl formate) and retro-aldol (**4a** to oxaloacetate and **2e**), oxidation (**2b** to glyoxylate) and reduction (fumaroyl formate to **2d** and oxaloacetate to **3a**), hydrolysis (**1a** to **2c**), and decarboxylation (**2c** to **2e**).

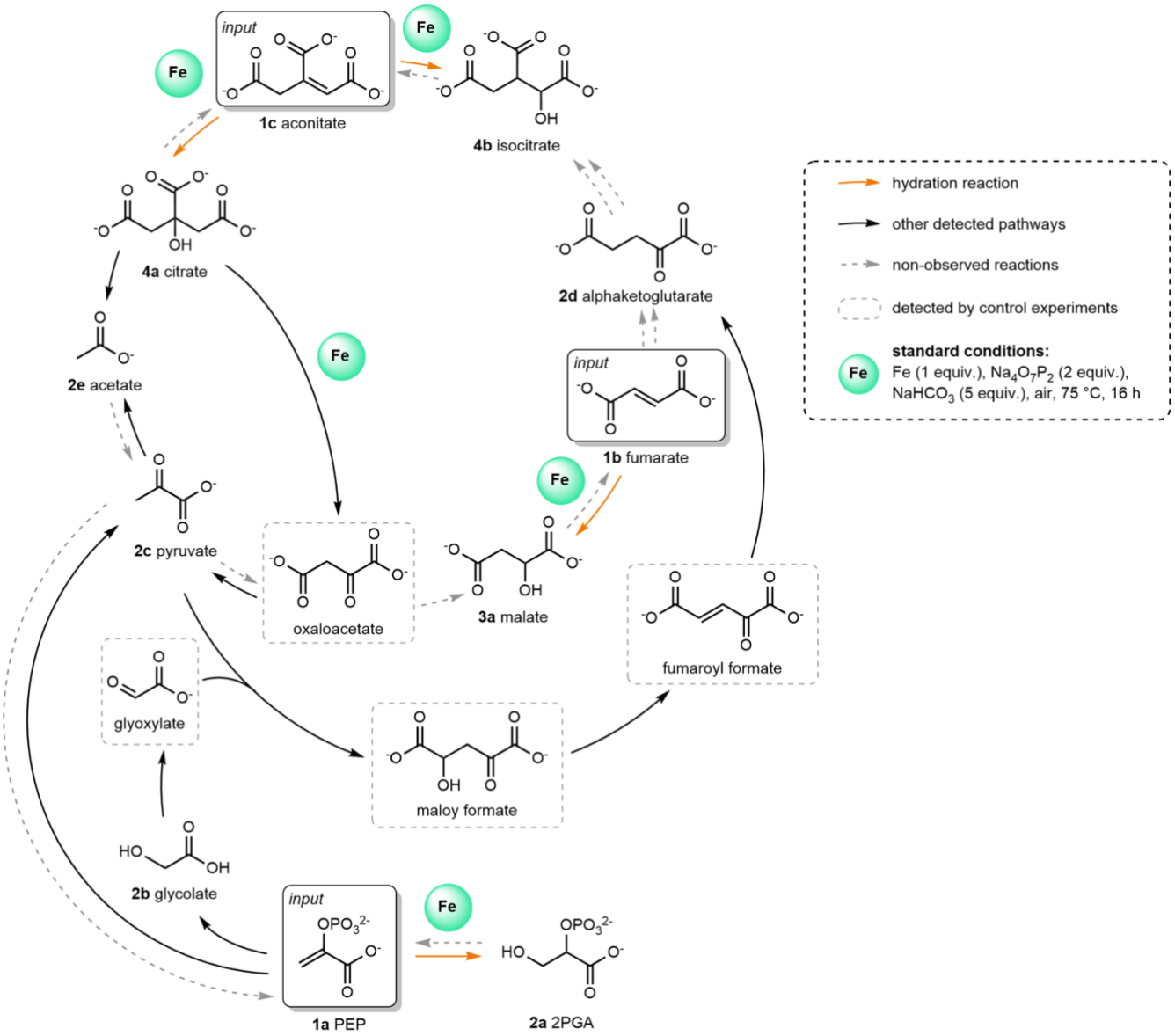

Figure 7. The non-enzymatic reaction network is generated from the hydration of key metabolites (i.e., PEP, aconitate, and fumarate). **1a**; **1b**, and **1c** were added simultaneously in a one-pot manner and products **2a**-**2e**, **3a** and **4a**-**4b** were detected by ^{1}H qNMR (for details, see Table S17). Products in dashed grey boxes were not detected directly by ^{1}H NMR within the reaction network but observed via control experiments (for details, see Fig. S18, S20 and S28C).

Prebiotic relevance of this study

Our study shows that all hydration reactions found in the rTCA cycle and gluconeogenesis can occur under a common set of mild nonenzymatic conditions (25-75 °C in aqueous bicarbonate solution). The reaction works under oxidative conditions in the presence of a reduced iron source (either Fe^{0}, Fe^{2+}, or green rust) and pyrophosphate, components that can be found on early Earth.

Although the steady state concentration of O_2 in the prebiotic atmosphere is thought to have been very low, several studies now show that O_2 was locally produced continuously on the Archean earth by mechanochemical water splitting due to turbulent water flow over minerals,[65,66] or due to radiolysis of water by ionizing radiation of ^{40}K isotopes.[67] All of these studies also report the formation of reactive oxygen species (ROS) such as H_2O_2 and hydroxyl radicals, prior to the formation of O_2. Among the various ways to form ROS, for instance by photolysis

of atmospheric water vapor[68,69] or by harnessing the properties of the water-air interface of aqueous microdroplet,[70,71] the ones reported at mineral-water interfaces are of particular interest. Indeed, several studies demonstrated that ROS could be formed on natural abundant sulfide minerals[72] such as pyrite,[73–76] which is proposed as a mineral of prime interest for the origin of life.[3,77–79] Interestingly, these studies showed the formation of ROS in anaerobic environment using abundant minerals containing iron[73–76] and silicates[65,66] naturally found in hydrothermal vents.[3,80–82] Such environments present basic pH[82] and a temperature range of 25 to 125 °C,[81,83] both compatible with the conditions reported in this study for alkene hydration.

Another key element of the reported conditions is pyrophosphate. Polyphosphates such as pyrophosphate are thought to have been produced by geochemical processes on the early Earth.[84–87] Interestingly, it was reported that pyrophosphate could be formed through the oxidation of reduced phosphorous (HPO_3^{2-} or $H_2PO_2^-$) in the presence of H_2O_2.[84] In this study, pyrophosphate was used as a chelating agent for iron species, also under oxidative conditions, potentially preventing the formation of iron precipitates in solution,[49] and allowing the nonenzymatic hydration of core metabolites.

Lastly, the key promoter of the reaction is an iron-based species. Iron is of particular interest because it is one of the most abundant metals on Earth,[88] plays fundamental roles in biology,[30] and has been shown to be among the most efficient in promoting nonenzymatic metabolic reactions.[11,15,16,20,89–95] Notably, iron can be naturally found in the form of green rust, a mixture of Fe(II)/Fe(III) hydroxy salts. In this study, green rust was found to be a suitable source of iron for the reaction. Of particular interest is that the reported conditions are closely related to those that form carbonate green rust, which is thought to have covered the surface of the primitive ocean,[44] and has been proposed as an "organizing seed" for the emergence of life.[44,96]

Conclusion

We report mild nonenzymatic conditions (25-75 °C in aqueous bicarbonate solution) for all hydration reactions in the rTCA cycle, gluconeogenesis, and on metabolites from other pathways. Notably, the nonenzymatic hydration of **PEP** to **2PGA** was reported for the first time. The conditions also enable a nonenzymatic version of the retro-aldol reaction of citrate found in the rTCA cycle, which was so far only reported in aqueous microdroplets. The conditions rely on a combination of a reduced iron source (either Fe^0, Fe^{2+}, or green rust), pyrophosphate, bicarbonate, and oxygen.

Preliminary mechanistic insights indicate that the reaction depends on at least one open-shell species and the slow formation of an active iron species. The hydration occurs exclusively on α,β-unsaturated carboxylate groups, and does so with a mild preference for the formation of the C-O bond at the least substituted carbon. The hydration reactions of the rTCA cycle and gluconeogenesis were found to all occur simultaneously with dehydration, (retro)aldol, oxidation/reduction, hydrolysis, and decarboxylation in the same pot under a common set of mild nonenzymatic conditions.

The present results are part of a larger effort to triangulate the conditions under which chemistry might self-organize into a complex chemical reaction network (i.e. a protometabolism). In contrast to previous efforts to search

for conditions relevant to reactions within a single metabolic pathway, here we took a complementary approach by screening for nonenzymatic conditions for reaction classes that transcend pathways. Future efforts to investigate by reaction class, rather than pathway, should continue to narrow the search.

Acknowledgements

This work was supported by the Interdisciplinary Thematic Institute ITI-CSC via the IdEx Unistra (ANR-10-IDEX-0002) within the program Investissement d'Avenir. J.Z. thanks the French government for an MRT fellowship. This project has received funding from the European Research Council (ERC) under the European Union's Horizon 2020 research and innovation program (grant agreement no. 101001752). J.M. thanks the VW Foundation (no. 96_742) for generous support. Dr. Robert J Mayer, Dr. Quentin Dherbassy and Dr. Emilie Werner are thanked for helpful discussions.

References

(1) Weiss, M. C.; Sousa, F. L.; Mrnjavac, N.; Neukirchen, S.; Roettger, M.; Nelson-Sathi, S.; Martin, W. F. The Physiology and Habitat of the Last Universal Common Ancestor. *Nat Microbiol* **2016**, *1* (9), 16116. https://doi.org/10.1038/nmicrobiol.2016.116.

(2) Wachtershauser, G. Evolution of the First Metabolic Cycles. *Proceedings of the National Academy of Sciences* **1990**, *87* (1), 200–204. https://doi.org/10.1073/pnas.87.1.200.

(3) Martin, W.; Russell, M. J. On the Origin of Biochemistry at an Alkaline Hydrothermal Vent. *Philos Trans R Soc Lond B Biol Sci* **2007**, *362* (1486), 1887–1926. https://doi.org/10.1098/rstb.2006.1881.

(4) Harrison, S. A.; Lane, N. Life as a Guide to Prebiotic Nucleotide Synthesis. *Nat Commun* **2018**, *9* (1), 5176. https://doi.org/10.1038/s41467-018-07220-y.

(5) Ralser, M. An Appeal to Magic? The Discovery of a Non-Enzymatic Metabolism and Its Role in the Origins of Life. *Biochemical Journal* **2018**, *475* (16), 2577–2592. https://doi.org/10.1042/BCJ20160866.

(6) Muchowska, K. B.; Varma, S. J.; Moran, J. Nonenzymatic Metabolic Reactions and Life's Origins. *Chem. Rev.* **2020**, *120* (15), 7708–7744. https://doi.org/10.1021/acs.chemrev.0c00191.

(7) Harrison, S. A.; Rammu, H.; Liu, F.; Halpern, A.; Nunes Palmeira, R.; Lane, N. Life as a Guide to Its Own Origins. *Annual Review of Ecology, Evolution, and Systematics* **2023**, *54* (1), 327–350. https://doi.org/10.1146/annurev-ecolsys-110421-101509.

(8) Hartman, H. Speculations on the Origin and Evolution of Metabolism. *J Mol Evol* **1975**, *4* (4), 359–370. https://doi.org/10.1007/BF01732537.

(9) Morowitz, H. J. A Theory of Biochemical Organization, Metabolic Pathways, and Evolution. *Complexity* **1999**, *4*. https://doi.org/10.1002/(SICI)1099-0526(199907/08)4:6<39::AID-CPLX8>3.0.CO;2-2.

(10) Smith, E.; Morowitz, H. J. *The Origin and Nature of Life on Earth: The Emergence of the Fourth Geosphere*; Cambridge University Press, 2016.

(11) Keller, M. A.; Zylstra, A.; Castro, C.; Turchyn, A. V.; Griffin, J. L.; Ralser, M. Conditional Iron and pH-Dependent Activity of a Non-Enzymatic Glycolysis and Pentose Phosphate Pathway. *Science Advances* **2016**, *2* (1), e1501235. https://doi.org/10.1126/sciadv.1501235.

(12) Messner, C. B.; Driscoll, P. C.; Piedrafita, G.; Volder, M. F. L. D.; Ralser, M. Nonenzymatic Gluconeogenesis-like Formation of Fructose 1,6-Bisphosphate in Ice. *PNAS* **2017**, *114* (28), 7403–7407. https://doi.org/10.1073/pnas.1702274114.

(13) Laurino, P.; Tawfik, D. S. Spontaneous Emergence of S-Adenosylmethionine and the Evolution of Methylation. *Angew Chem Int Ed Engl* **2017**, *56* (1), 343–345. https://doi.org/10.1002/anie.201609615.

(14) Akouche, M.; Jaber, M.; Maurel, M.-C.; Lambert, J.-F.; Georgelin, T. Phosphoribosyl Pyrophosphate: A Molecular Vestige of the Origin of Life on Minerals. *Angewandte Chemie International Edition* **2017**, *56* (27), 7920–7923. https://doi.org/10.1002/anie.201702633.

(15) Muchowska, K. B.; Varma, S. J.; Chevallot-Beroux, E.; Lethuillier-Karl, L.; Li, G.; Moran, J. Metals Promote Sequences of the Reverse Krebs Cycle. *Nat Ecol Evol* **2017**, *1* (11), 1716–1721. https://doi.org/10.1038/s41559-017-0311-7.

(16) Varma, S. J.; Muchowska, K. B.; Chatelain, P.; Moran, J. Native Iron Reduces CO2 to Intermediates and End-Products of the Acetyl-CoA Pathway. *Nat Ecol Evol* **2018**, *2* (6), 1019–1024. https://doi.org/10.1038/s41559-018-0542-2.

(17) Springsteen, G.; Yerabolu, J. R.; Nelson, J.; Rhea, C. J.; Krishnamurthy, R. Linked Cycles of Oxidative Decarboxylation of Glyoxylate as Protometabolic Analogs of the Citric Acid Cycle. *Nat Commun* **2018**, *9* (1), 91. https://doi.org/10.1038/s41467-017-02591-0.

(18) Muchowska, K. B.; Varma, S. J.; Moran, J. Synthesis and Breakdown of Universal Metabolic Precursors Promoted by Iron. *Nature* **2019**, *569* (7754), 104–107. https://doi.org/10.1038/s41586-019-1151-1.

(19) Barge, L. M.; Flores, E.; Baum, M. M.; VanderVelde, D. G.; Russell, M. J. Redox and pH Gradients Drive Amino Acid Synthesis in Iron Oxyhydroxide Mineral Systems. *Proc Natl Acad Sci U S A* **2019**, *116* (11), 4828–4833. https://doi.org/10.1073/pnas.1812098116.

(20) Preiner, M.; Igarashi, K.; Muchowska, K. B.; Yu, M.; Varma, S. J.; Kleinermanns, K.; Nobu, M. K.; Kamagata, Y.; Tüysüz, H.; Moran, J.; Martin, W. F. A Hydrogen-Dependent Geochemical Analogue of Primordial Carbon and Energy Metabolism. *Nat Ecol Evol* **2020**, *4* (4), 534–542. https://doi.org/10.1038/s41559-020-1125-6.

(21) Mayer, R. J.; Kaur, H.; Rauscher, S. A.; Moran, J. Mechanistic Insight into Metal Ion-Catalyzed Transamination. *J Am Chem Soc* **2021**, *143* (45), 19099–19111. https://doi.org/10.1021/jacs.1c08535.

(22) Yi, J.; Kaur, H.; Kazöne, W.; Rauscher, S. A.; Gravillier, L.-A.; Muchowska, K. B.; Moran, J. A Nonenzymatic Analog of Pyrimidine Nucleobase Biosynthesis. *Angewandte Chemie International Edition* **2022**, *61* (23), e202117211. https://doi.org/10.1002/anie.202117211.

(23) Rauscher, S. A.; Moran, J. Hydrogen Drives Part of the Reverse Krebs Cycle under Metal or Meteorite Catalysis. *Angewandte Chemie International Edition* **2022**, *61* (51), e202212932. https://doi.org/10.1002/anie.202212932.

(24) Harrison, S. A.; Webb, W. L.; Rammu, H.; Lane, N. Prebiotic Synthesis of Aspartate Using Life's Metabolism as a Guide. *Life* **2023**, *13* (5), 1177. https://doi.org/10.3390/life13051177.

(25) Hudson, R.; de Graaf, R.; Strandoo Rodin, M.; Ohno, A.; Lane, N.; McGlynn, S. E.; Yamada, Y. M. A.; Nakamura, R.; Barge, L. M.; Braun, D.; Sojo, V. CO2 Reduction Driven by a pH Gradient. *Proc Natl Acad Sci U S A* **2020**, *117* (37), 22873–22879. https://doi.org/10.1073/pnas.2002659117.

(26) Beyazay, T.; Belthle, K. S.; Farès, C.; Preiner, M.; Moran, J.; Martin, W. F.; Tüysüz, H. Ambient Temperature CO2 Fixation to Pyruvate and Subsequently to Citramalate over Iron and Nickel Nanoparticles. *Nat Commun* **2023**, *14* (1), 570. https://doi.org/10.1038/s41467-023-36088-w.

(27) McMurry, J. E.; Begley, T. P. *The Organic Chemistry of Biological Pathways*, Second edition.; W. H. Freeman: Greenwood Village, Colorado, 2015.

(28) Smith, E.; Morowitz, H. J. Universality in Intermediary Metabolism. *PNAS* **2004**, *101* (36), 13168–13173. https://doi.org/10.1073/pnas.0404922101.

(29) Miller, S. L.; Smith-Magowan, D. The Thermodynamics of the Krebs Cycle and Related Compounds. *Journal of Physical and Chemical Reference Data* **1990**, *19* (4), 1049–1073. https://doi.org/10.1063/1.555878.

(30) Flint, D. H.; Allen, R. M. Iron−Sulfur Proteins with Nonredox Functions. *Chem. Rev.* **1996**, *96* (7), 2315–2334. https://doi.org/10.1021/cr950041r.

(31) Beinert, H.; Kennedy, M. C.; Stout, C. D. Aconitase as Iron−Sulfur Protein, Enzyme, and Iron-Regulatory Protein. *Chem. Rev.* **1996**, *96* (7), 2335–2374. https://doi.org/10.1021/cr950040z.

(32) Chen, B.-S.; Otten, L. G.; Hanefeld, U. Stereochemistry of Enzymatic Water Addition to C=C Bonds. *Biotechnology Advances* **2015**, *33* (5), 526–546. https://doi.org/10.1016/j.biotechadv.2015.01.007.

(33) Lebioda, L.; Stec, B. Mechanism of Enolase: The Crystal Structure of Enolase-Magnesium-2-Phosphoglycerate/Phosphoenolpyruvate Complex at 2.2-.ANG. Resolution. *Biochemistry* **1991**, *30* (11), 2817–2822. https://doi.org/10.1021/bi00225a012.

(34) Greinert, T.; Vogel, K.; Seifert, A. I.; Siewert, R.; Andreeva, I. V.; Verevkin, S. P.; Maskow, T.; Sadowski, G.; Held, C. Standard Gibbs Energy of Metabolic Reactions: V. Enolase Reaction. *Biochimica et Biophysica Acta (BBA) - Proteins and Proteomics* **2020**, *1868* (4), 140365. https://doi.org/10.1016/j.bbapap.2020.140365.

(35) Reed, G. H.; Poyner, R. R.; Larsen, T. M.; Wedekind, J. E.; Rayment, I. Structural and Mechanistic Studies of Enolase. *Curr Opin Struct Biol* **1996**, *6* (6), 736–743. https://doi.org/10.1016/s0959-440x(96)80002-9.

(36) Bender, M. L.; Connors, K. A. A Non-Enzymatic Olefinic Hydration under Neutral Conditions: The Kinetics and Mechanism of the Hydration of Fumaric Acid Monoanion. *J. Am. Chem. Soc.* **1962**, *84* (10), 1980–1986. https://doi.org/10.1021/ja00869a041.

(37) Rozelle, L. T.; Alberty, R. A. Kinetics of the Acid Catalysis of the Hydration of Fumaric Acid to Malic Acid. *J. Phys. Chem.* **1957**, *61* (12), 1637–1640. https://doi.org/10.1021/j150558a017.

(38) Yadav, M.; Pulletikurti, S.; Yerabolu, J. R.; Krishnamurthy, R. Cyanide as a Primordial Reductant Enables a Protometabolic Reductive Glyoxylate Pathway. *Nat. Chem.* **2022**, *14* (2), 170–178. https://doi.org/10.1038/s41557-021-00878-w.

(39) Ju, Y.; Zhang, H.; Jiang, Y.; Wang, W.; Kan, G.; Yu, K.; Wang, X.; Liu, J.; Jiang, J. Aqueous Microdroplets Promote C–C Bond Formation and Sequences in the Reverse Tricarboxylic Acid Cycle. *Nat Ecol Evol* **2023**, *7* (11), 1892–1902. https://doi.org/10.1038/s41559-023-02193-8.

(40) Wei, H.; Vejerano, E. P.; Leng, W.; Huang, Q.; Willner, M. R.; Marr, L. C.; Vikesland, P. J. Aerosol Microdroplets Exhibit a Stable pH Gradient. *Proceedings of the National Academy of Sciences* **2018**, *115* (28), 7272–7277. https://doi.org/10.1073/pnas.1720488115.

(41) Benkovic, S. J.; Schray, K. J. Kinetics and Mechanisms of Phosphoenolpyruvate Hydrolysis. *Biochemistry* **1968**, *7* (11), 4090–4096. https://doi.org/10.1021/bi00851a043.

(42) Benkovic, S. J.; Schray, K. J. Metal Ion Catalysis of Phosphoryl Transfer from Phosphoenolpyruvate. *Biochemistry* **1968**, *7* (11), 4097–4102. https://doi.org/10.1021/bi00851a044.

(43) Benkovic, S. J.; Schray, K. J. Mechanisms of Hydrolysis of Phosphate Ester Derivatives of Phosphoenolpyruvic Acid. *J. Am. Chem. Soc.* **1971**, *93* (10), 2522–2529. https://doi.org/10.1021/ja00739a027.

(44) Russell, M. J. Green Rust: The Simple Organizing ‘Seed’ of All Life? *Life* **2018**, *8* (3), 35. https://doi.org/10.3390/life8030035.

(45) Gahan, L. R.; Harrowfield, J. M.; Herlt, A. J.; Lindoy, L. F.; Whimp, P. O.; Sargeson, A. W. Metal Ion Promoted Hydration of Pendant Alkenes and Its Possible Relationship to Aconitase. *J. Am. Chem. Soc.* **1985**, *107* (22), 6231–6242. https://doi.org/10.1021/ja00308a015.

(46) Olson, M. V.; Taube, H. Hydration and Isomerization of Coordinated Maleate. *J. Am. Chem. Soc.* **1970**, *92* (10), 3236–3237. https://doi.org/10.1021/ja00713a081.

(47) Pa Ho Hsu. Comparison of Iron(III) and Aluminum in Precipitation of Phosphate from Solution. *Water Research* **1976**, *10* (10), 903–907. https://doi.org/10.1016/0043-1354(76)90026-9.

(48) de Zwart, I. I.; Meade, S. J.; Pratt, A. J. Biomimetic Phosphoryl Transfer Catalysed by Iron(II)-Mineral Precipitates. *Geochimica et Cosmochimica Acta* **2004**, *68* (20), 4093–4098. https://doi.org/10.1016/j.gca.2004.01.028.

(49) Kim, H.-H.; Lee, H.; Kim, H.-E.; Seo, J.; Hong, S. W.; Lee, J.-Y.; Lee, C. Polyphosphate-Enhanced Production of Reactive Oxidants by Nanoparticulate Zero-Valent Iron and Ferrous Ion in the Presence of Oxygen: Yield and Nature of Oxidants. *Water Research* **2015**, *86*, 66–73. https://doi.org/10.1016/j.watres.2015.06.016.

(50) Wang, L.; Wang, F.; Li, P.; Zhang, L. Ferrous–Tetrapolyphosphate Complex Induced Dioxygen Activation for Toxic Organic Pollutants Degradation. *Separation and Purification Technology* **2013**, *120*, 148–155. https://doi.org/10.1016/j.seppur.2013.10.002.

(51) Wang, L.; Cao, M.; Ai, Z.; Zhang, L. Dramatically Enhanced Aerobic Atrazine Degradation with Fe@Fe $_2$ O $_3$ Core–Shell Nanowires by Tetrapolyphosphate. *Environ. Sci. Technol.* **2014**, *48* (6), 3354–3362. https://doi.org/10.1021/es404741x.

(52) Abdelmoula, M.; Refait, Ph.; Drissi, S. H.; Mihe, J. P.; Génin, J.-M. R. Conversion Electron Mössbauer Spectroscopy and X-Ray Diffraction Studies of the Formation of Carbonate-Containing Green Rust One by Corrosion of Metallic Iron in NaHCO3 and (NaHCO3 + NaCl) Solutions. *Corrosion Science* **1996**, *38* (4), 623–633. https://doi.org/10.1016/0010-938X(95)00153-B.

(53) Stubbs, R. T.; Yadav, M.; Krishnamurthy, R.; Springsteen, G. A Plausible Metal-Free Ancestral Analogue of the Krebs Cycle Composed Entirely of α-Ketoacids. *Nat. Chem.* **2020**, *12* (11), 1016–1022. https://doi.org/10.1038/s41557-020-00560-7.

(54) Kaur, H.; Rauscher, S. A.; Werner, E.; Song, Y.; Yi, J.; Kazöne, W.; Martin, W. F.; Tüysüz, H.; Moran, J. A Prebiotic Krebs Cycle Analog Generates Amino Acids with H2 and NH3 over Nickel. *Chem* **2024**. https://doi.org/10.1016/j.chempr.2024.02.001.

(55) Kachur, A. V.; Tuttle, S. W.; Biaglow, J. E. Autoxidation of Ferrous Ion Complexes: A Method for the Generation of Hydroxyl Radicals. *Radiat Res* **1998**, *150* (4), 475–482.

(56) Morgan, B.; Lahav, O. The Effect of pH on the Kinetics of Spontaneous Fe(II) Oxidation by O2 in Aqueous Solution – Basic Principles and a Simple Heuristic Description. *Chemosphere* **2007**, *68* (11), 2080–2084. https://doi.org/10.1016/j.chemosphere.2007.02.015.

(57) Keenan, C. R.; Sedlak, D. L. Factors Affecting the Yield of Oxidants from the Reaction of Nanoparticulate Zero-Valent Iron and Oxygen. *Environ. Sci. Technol.* **2008**, *42* (4), 1262–1267. https://doi.org/10.1021/es7025664.

(58) Fenton, H. J. H. LXXIII.—Oxidation of Tartaric Acid in Presence of Iron. *J. Chem. Soc., Trans.* **1894**, *65* (0), 899–910. https://doi.org/10.1039/CT8946500899.

(59) Coggins, A. J.; Powner, M. W. Prebiotic Synthesis of Phosphoenol Pyruvate by α-Phosphorylation-Controlled Triose Glycolysis. *Nature Chem* **2017**, *9* (4), 310–317. https://doi.org/10.1038/nchem.2624.

(60) Yao, H.; Richardson, D. E. Epoxidation of Alkenes with Bicarbonate-Activated Hydrogen Peroxide. *J. Am. Chem. Soc.* **2000**, *122* (13), 3220–3221. https://doi.org/10.1021/ja993935s.

(61) Wang, Z.; Cui, Y.-T.; Xu, Z.-B.; Qu, J. Hot Water-Promoted Ring-Opening of Epoxides and Aziridines by Water and Other Nucleopliles. *J. Org. Chem.* **2008**, *73* (6), 2270–2274. https://doi.org/10.1021/jo702401t.

(62) Ruby, C.; Abdelmoula, M.; Naille, S.; Renard, A.; Khare, V.; Ona-Nguema, G.; Morin, G.; Génin, J.-M. R. Oxidation Modes and Thermodynamics of FeII–III Oxyhydroxycarbonate Green Rust: Dissolution–Precipitation versus *in Situ* Deprotonation. *Geochimica et Cosmochimica Acta* **2010**, *74* (3), 953–966. https://doi.org/10.1016/j.gca.2009.10.030.

(63) Génin, J.-M. R.; Ruby, C.; Géhin, A.; Refait, P. Synthesis of Green Rusts by Oxidation of of Fe(OH)2, their Products of Oxidation and Reduction of Ferric Oxyhydroxides; E_h–pH Pourbaix diagrams, *Comptes Rendus Geoscience* **2006**, *338* (6), 433–446. https://doi.org/10.1016/j.crte.2006.04.004.

(64) Tran, Q. P.; Adam, Z. R.; Fahrenbach, A. C. Prebiotic Reaction Networks in Water. *Life (Basel)* **2020**, *10* (12), 352. https://doi.org/10.3390/life10120352.

(65) He, H.; Wu, X.; Xian, H.; Zhu, J.; Yang, Y.; Lv, Y.; Li, Y.; Konhauser, K. O. An Abiotic Source of Archean Hydrogen Peroxide and Oxygen That Pre-Dates Oxygenic Photosynthesis. *Nat Commun* **2021**, *12* (1), 6611. https://doi.org/10.1038/s41467-021-26916-2.

(66) He, H.; Wu, X.; Zhu, J.; Lin, M.; Lv, Y.; Xian, H.; Yang, Y.; Lin, X.; Li, S.; Li, Y.; Teng, H. H.; Thiemens, M. H. A Mineral-Based Origin of Earth's Initial Hydrogen Peroxide and Molecular Oxygen. *Proceedings of the National Academy of Sciences* **2023**, *120* (13), e2221984120. https://doi.org/10.1073/pnas.2221984120.

(67) Draganić, I. G.; Bjergbakke, E.; Draganić, Z. D.; Sehested, K. Decomposition of Ocean Waters by Potassium-40 Radiation 3800 Ma Ago as a Source of Oxygen and Oxidizing Species. *Precambrian Research* **1991**, *52* (3), 337–345. https://doi.org/10.1016/0301-9268(91)90087-Q.

(68) Vander Wood, T. B.; Thiemens, M. H. The Fate of the Hydroxyl Radical in the Earth's Primitive Atmosphere and Implications for the Production of Molecular Oxygen. *Journal of Geophysical Research: Oceans* **1980**, *85* (C3), 1605–1610. https://doi.org/10.1029/JC085iC03p01605.

(69) Kroll, J. A.; Frandsen, B. N.; Kjaergaard, H. G.; Vaida, V. Atmospheric Hydroxyl Radical Source: Reaction of Triplet SO2 and Water. *J. Phys. Chem. A* **2018**, *122* (18), 4465–4469. https://doi.org/10.1021/acs.jpca.8b03524.

(70) Lee, J. K.; Walker, K. L.; Han, H. S.; Kang, J.; Prinz, F. B.; Waymouth, R. M.; Nam, H. G.; Zare, R. N. Spontaneous Generation of Hydrogen Peroxide from Aqueous Microdroplets. *Proceedings of the National Academy of Sciences* **2019**, *116* (39), 19294–19298. https://doi.org/10.1073/pnas.1911883116.

(71) Lee, J. K.; Han, H. S.; Chaikasetsin, S.; Marron, D. P.; Waymouth, R. M.; Prinz, F. B.; Zare, R. N. Condensing Water Vapor to Droplets Generates Hydrogen Peroxide. *Proceedings of the National Academy of Sciences* **2020**, *117* (49), 30934–30941. https://doi.org/10.1073/pnas.2020158117.

(72) Javadi Nooshabadi, A.; Hanumantha Rao, K. Formation of Hydrogen Peroxide by Sulphide Minerals. *Hydrometallurgy* **2014**, *141*, 82–88. https://doi.org/10.1016/j.hydromet.2013.10.011.

(73) Guo, H.; Li, Y.; Li, Y.; Liao, M.; Lai, Y. Generation of Reactive Oxygen Species on Pyrite Surfaces: A Likely Oxidation Mechanism for near-Vent, Hydrothermal Fluid-Dominated BIFs. *Chemical Geology* **2020**, *551*, 119766. https://doi.org/10.1016/j.chemgeo.2020.119766.

(74) Xu, J.; Sahai, N.; Eggleston, C. M.; Schoonen, M. A. A. Reactive Oxygen Species at the Oxide/Water Interface: Formation Mechanisms and Implications for Prebiotic Chemistry and the Origin of Life. *Earth and Planetary Science Letters* **2013**, *363*, 156–167. https://doi.org/10.1016/j.epsl.2012.12.008.

(75) Xian, H.; Zhu, J.; Tan, W.; Tang, H.; Liu, P.; Zhu, R.; Liang, X.; Wei, J.; He, H.; Teng, H. H. The Mechanism of Defect Induced Hydroxylation on Pyrite Surfaces and Implications for Hydroxyl Radical Generation in Prebiotic Chemistry. *Geochimica et Cosmochimica Acta* **2019**, *244*, 163–172. https://doi.org/10.1016/j.gca.2018.10.009.

(76) Borda, M. J.; Elsetinow, A. R.; Schoonen, M. A.; Strongin, D. R. Pyrite-Induced Hydrogen Peroxide Formation as a Driving Force in the Evolution of Photosynthetic Organisms on an Early Earth. *Astrobiology* **2001**, *1* (3), 283–288. https://doi.org/10.1089/15311070152757474.

(77) Russell, M. J.; Hall, A. J.; Gize, A. P. Pyrite and the Origin of Life. *Nature* **1990**, *344* (6265), 387–387. https://doi.org/10.1038/344387b0.

(78) Wächtershäuser, G. Before Enzymes and Templates: Theory of Surface Metabolism. *Microbiological Reviews* **1988**, *52* (4), 452–484. https://doi.org/10.1128/MMBR.52.4.452-484.1988.

(79) Russell, M. J.; Daniel, R. M.; Hall, A. J.; Sherringham, J. A. A Hydrothermally Precipitated Catalytic Iron Sulphide Membrane as a First Step toward Life. *J Mol Evol* **1994**, *39* (3), 231–243. https://doi.org/10.1007/BF00160147.

(80) Tosca, N. J.; Tutolo, B. M. Hydrothermal Vent Fluid-Seawater Mixing and the Origins of Archean Iron Formation. *Geochimica et Cosmochimica Acta* **2023**, *352*, 51–68. https://doi.org/10.1016/j.gca.2023.05.002.

(81) Sojo, V.; Herschy, B.; Whicher, A.; Camprubí, E.; Lane, N. The Origin of Life in Alkaline Hydrothermal Vents. *Astrobiology* **2016**, *16* (2), 181–197. https://doi.org/10.1089/ast.2015.1406.

(82) Russell, M. J.; Hall, A. J.; Martin, W. Serpentinization as a Source of Energy at the Origin of Life. *Geobiology* **2010**, *8* (5), 355–371. https://doi.org/10.1111/j.1472-4669.2010.00249.x.

(83) Seyfried, W. E.; Pester, N. J.; Tutolo, B. M.; Ding, K. The Lost City Hydrothermal System: Constraints Imposed by Vent Fluid Chemistry and Reaction Path Models on Subseafloor Heat and Mass Transfer Processes. *Geochimica et Cosmochimica Acta* **2015**, *163*, 59–79. https://doi.org/10.1016/j.gca.2015.04.040.

(84) Pasek, M. A.; Kee, T. P.; Bryant, D. E.; Pavlov, A. A.; Lunine, J. I. Production of Potentially Prebiotic Condensed Phosphates by Phosphorus Redox Chemistry. *Angewandte Chemie* **2008**, *120* (41), 8036–8038. https://doi.org/10.1002/ange.200802145.

(85) Yamagata, Y.; Watanabe, H.; Saitoh, M.; Namba, T. Volcanic Production of Polyphosphates and Its Relevance to Prebiotic Evolution. *Nature* **1991**, *352* (6335), 516–519. https://doi.org/10.1038/352516a0.

(86) Britvin, S. N.; Murashko, M. N.; Vapnik, Y.; Vlasenko, N. S.; Krzhizhanovskaya, M. G.; Vereshchagin, O. S.; Bocharov, V. N.; Lozhkin, M. S. Cyclophosphates, a New Class of Native Phosphorus Compounds, and Some Insights into Prebiotic Phosphorylation on Early Earth. *Geology* **2021**, *49* (4), 382–386. https://doi.org/10.1130/G48203.1.

(87) Pasek, M. A.; Lauretta, D. S. Aqueous Corrosion of Phosphide Minerals from Iron Meteorites: A Highly Reactive Source of Prebiotic Phosphorus on the Surface of the Early Earth. *Astrobiology* **2005**, *5* (4), 515–535. https://doi.org/10.1089/ast.2005.5.515.

(88) *Abundance of Elements in the Earth's Crust and in the Sea. In CRC Handbook of Chemistry and Physics; Rumble, J. R., Ed.; CRC Press/Taylor & Francis: Boca Raton, FL, 2016; Pp 14−17*.

(89) Werner, E.; Pinna, S.; Mayer, R. J.; Moran, J. Metal/ADP Complexes Promote Phosphorylation of Ribonucleotides. *J. Am. Chem. Soc.* **2023**, *145* (39), 21630–21637. https://doi.org/10.1021/jacs.3c08047.

(90) Dherbassy, Q.; Mayer, R. J.; Muchowska, K. B.; Moran, J. Metal-Pyridoxal Cooperativity in Nonenzymatic Transamination. *J. Am. Chem. Soc.* **2023**, *145* (24), 13357–13370. https://doi.org/10.1021/jacs.3c03542.

(91) Mayer, R.; Moran, J. Metal Ions Turn on a Stereoselective Nonenzymatic Reduction of Keto Acids by the Coenzyme NADH. ChemRxiv October 10, **2023**. https://doi.org/10.26434/chemrxiv-2023-jdhxk.

(92) Henriques Pereira, D. P.; Leethaus, J.; Beyazay, T.; Do Nascimento Vieira, A.; Kleinermanns, K.; Tüysüz, H.; Martin, W. F.; Preiner, M. Role of Geochemical Protoenzymes (Geozymes) in Primordial Metabolism: Specific Abiotic Hydride Transfer by Metals to the Biological Redox Cofactor NAD^+. *The FEBS Journal* **2022**, *289* (11), 3148–3162. https://doi.org/10.1111/febs.16329.

(93) Keller, M. A.; Turchyn, A. V.; Ralser, M. Non-Enzymatic Glycolysis and Pentose Phosphate Pathway-like Reactions in a Plausible Archean Ocean. *Molecular Systems Biology* **2014**, *10* (4), 725. https://doi.org/10.1002/msb.20145228.

(94) Brabender, M.; Henriques Pereira, D. P.; Mrnjavac, N.; Schlikker, M. L.; Kimura, Z.-I.; Sucharitakul, J.; Kleinermanns, K.; Tüysüz, H.; Buckel, W.; Preiner, M.; Martin, W. F. Ferredoxin Reduction by Hydrogen with Iron Functions as an Evolutionary Precursor of Flavin-Based Electron Bifurcation. *Proceedings of the National Academy of Sciences* **2024**, *121* (13), e2318969121. https://doi.org/10.1073/pnas.2318969121.

(95) Camprubi, E.; Jordan, S. F.; Vasiliadou, R.; Lane, N. Iron Catalysis at the Origin of Life. *IUBMB Life* **2017**, *69* (6), 373–381. https://doi.org/10.1002/iub.1632.

(96) Branscomb, E.; Russell, M. J. Frankenstein or a Submarine Alkaline Vent: Who Is Responsible for Abiogenesis? *BioEssays* **2018**, *40* (8), 1700182. https://doi.org/10.1002/bies.201700182.